Electrocardiographic imaging (ECGI): a new noninvasive imaging modality for cardiac electrophysiology and arrhythmia

Dr. Yoram Rudy, Ph.D., F.A.H.A.
Cardiac Bioelectricity and Arrhythmia Center (CBAC)
Washington University in St. Louis
St. Louis, Missouri
U.S.A.

ABSTRACT

Cardiac arrhythmias are a major cause of death (7 million cases annually worldwide; 400,000 in the U.S. alone) and disability. Yet, a noninvasive imaging modality to identify patients at risk, provide accurate diagnosis and guide therapy is not yet available in clinical practice. In my conference presentation and proceedings article, I will describe examples of the application of Electrocardiographic Imaging (ECGI) in humans. ECGI is a new noninvasive imaging modality for cardiac arrhythmias developed in our laboratory. It combines recordings of 224 body-surface electrocardiograms and a thoracic CT scan to reconstruct potentials, electrograms and isochrones (activation sequences) on the heart surface. Examples include: (1) normal activation and repolarization; (2) activation during ventricular pacing; and (3) atrial flutter.

KEYWORDS: Cardiac arrhythmias, sudden death, electrocardiography, electrocardiographic imaging, inverse problem.

1. INTRODUCTION

More than 7 million people worldwide (400,000 in the U.S.) die annually from erratic heart rhythms and many more are disabled. Yet, there is no imaging modality, equivalent to CT or MRI, for identifying patients at risk, for providing accurate diagnosis, and for guiding therapy. At present, cardiac arrhythmias are diagnosed based on the ECG, which measures electric potentials on the body surface, far away from the heart. Such measurements suffer from low resolution and inadequate sensitivity and specificity. Importantly, the ECG cannot locate the arrhythmogenic substrate in the heart and, consequently, cannot be used to guide intervention. It is clear that a noninvasive imaging modality for cardiac arrhythmia is greatly needed for both clinical and research applications.

Electrocardiographic Imaging (ECGI) is a noninvasive imaging modality under development in our laboratory that reconstructs potentials, electrograms, and isochrones (activation sequences) on the surface of the heart. This method has been validated extensively in animal experiments and recently applied in human subjects [1]. In this conference proceeding, I will outline the ECGI method and provide examples of its application in humans.

2. THE ECGI METHODOLOGY

A multielectrode vest (or strips) is used to record simultaneously 224 body-surface electrocardiograms over the entire torso surface. This electrical information is the input data for ECGI. Following the ECG recordings, the subject undergoes a thoracic CT scan with the vest in position. The CT images provide the heart-surface geometry and vest-electrode positions. Together, the ECG mapping and CT imaging provide the electrical data and geometry data (the heart-torso geometrical relationship) that are required for ECGI. **Fig. 1** is a diagram of the ECGI procedure. All protocols were approved by the Institutional review Board (IRB) at University Hospitals of Cleveland.

Medical Imaging 2006: Physiology, Function, and Structure from Medical Images,
edited by Armando Manduca, Amir A. Amini, Proc. of SPIE Vol. 6143,
614306, (2006) · 1605-7422/06/$15 · doi: 10.1117/12.627964

Reconstruction of potentials on the epicardial surface of the heart from potentials measured on the body surface involves solving Laplace's equation in the source-free volume between the torso and epicardial surfaces [2-5]. We use an integral formulation of this problem (Green's Second Theorem) and the boundary element method (BEM) [6] to compute a matrix A that relates the torso potentials V_T to the epicardial potentials V_E; $V_T = AV_E$. Matrix A is derived from the heart-torso geometrical relationships as obtained from CT. It is an ill-pased matrix that cannot be inverted directly to computer V_E from measured V_T (the objective of ECGI). Stable solutions to this inverse problem are obtained using Tikhonov regularization methods [7] or the Generalized Minimal Residual (GMRes) iterative approach [8,9]. Once epicardial potentials are computed over the entire cardiac cycle (with time-resolution of 1 ms), these data can be used to construct epicardial electrograms (potential over time) at many points around the epicardium (we usually computer 600 electrograms). From the electrograms, the sequence of activation (isochrones) can be constructed by taking the point of steepest negative deflection on the QRS segment of each electrogram as the time of local activation. Similarly, recovery (repolarization) time is determined as the time of steepest positive deflection during the T-wave segment.

ECGI was validated extensively in canine heart experiments during normal sinus rhythm [10], ventricular pacing [11,12], abnormal activity in myocardial infarction [13], and reentrant ventricular tachycardia (VT) in infracted hearts [14,15]. It was also shown to image cardiac repolarization and its spatial dispersion, including repolarization abnormalities induced by regional cooling or warming of the myocardium [16]. Validation in humans included comparison to direct intraoperative mapping (using 200 epicardial electrodes) in patients undergoing open-heart surgery [17], and comparison to catheter mapping in a patient during VT [18].

3. EXAMPLES OF ECGI IMAGES

3.1 Normal ventricular activation (Fig. 2)

During normal activity (normal sinus rhythm), activation of the ventricular wall propagates from endocardium to epicardium in a broad wavefront [19]. Arrival of portion of the wavefront at the epicardial surface is termed "epicardial breakthrough" and generates a local potential minimum at that location [20]. The times and locations of epicardial breakthroughs provide important information on ventricular activation and its deviation from normal pattern in pathology. **Fig. 2a**, **left** shows a body surface potential map (the input data for ECGI) of a normal young adult at time 35 ms after the onset of QRS. **Fig. 2a, right** shows the epicardial potential map that was reconstructed from these body surface potentials using ECGI. Several local minima (dark blue and yellow, numbered 1, 2, 3, 4) reflect breakthrough sites. The earliest, termed "right ventricular breakthrough", occurs at the thinnest part of the right ventricular free wall (site 1); this minimum appears at 22 ms and intensifies at 35 ms. Several breakthrough sites are reconstructed on the left ventricular epicardium (sites 2, 3 and 4). The minimum at site 2 is breakthrough of an activation front generated by the left anterior fascicular branch of the left bundle branch of the specialized conduction system [21,22]. The minima at sites 1 and 2 were mapped directly during invasive mapping of chimpanzee hearts [23]. Site 3 is at the left ventricular apex and site 4 is in the posterior paraseptal region of the left ventricle. Invasive direct mapping has documented the occurrence of breakthroughs at all 4 epicardial sites, confirming the noninvasive reconstructions of ECGI [19,21,23].

Figure 2b, left shows noninvasively imaged electrograms from selected sites (1, 3, 4 and 5) on the epicardial surface. These noninvasive human electrograms show close similarity to those measured invasively in the chimpanzee from corresponding anatomical locations [23]. Electrograms of similar morphologies were also recorded during invasive human epicardial mapping studies [24,25]. The electrograms demonstrate that ECGI can reconstruct well epicardial T waves, reflecting repolarization. ECGI images of normal repolarization (Fig. 4 in reference 1; not shown here) show a static epicardial potential pattern during the entire T wave (very different from the dynamically changing patterns during activation). Anterior RV electrograms (location 1) show positive (upright) T waves, while posterior LV electrograms (location 4) show negative (inverted) T waves. A typical activation-recovery interval of 240 ms, which reflects the epicardial action potential duration [26], is computed from the ECGI reconstructed electrograms. This value is consistent with action potential duration measurements from human cardiac ventricular cells and tissue.

Fig. 2b, right shows a noninvasive isochrone map depicting the sequence of normal activation. Early activation occurs at four epicardial sites that correspond to the breakthroughs in **Fig. 2a**. The posterobasal LV is the last to activate (dark blue, posterior).

3.2 Activation during ventricular pacing (Fig. 3).

ECGI was conducted on a subject with an implanted biventricular pacing device. Images were reconstructed during RV pacing alone (**Fig. 3a,b**) and LV pacing alone (**Fig. 3c,d**). These protocols simulate focal arrhythmogenic activity, with the pacing sites simulating the ectopic foci (origins of the arrhythmogenic activity). For RV pacing (**Fig. 3a**) the site of earliest activation is surrounded by a region of negative potential (blue; **Fig. 3a, right map**) with an intense local minimum near the RV apex (asterisk). This minimum corresponds well with pacing lead terminal location as determined from CT (**Fig. 3a, left map**). The epicardial isochrone map (**Fig. 3b**) shows activation spread from the pacing site (red) superiorly to the rest of RV and apically toward the LV free wall. Lateral LV is last to activate (dark blue). As expected, electrograms near the pacing site show Q-wave morphology; at some distance QRS morphology; and far from the pacing site a positive R-wave. Similar patterns relative to the pacing site are reconstructed during LV pacing (**Fig. 3c** and **3d**). Compared with their location as determined from CT, ECGI located the RV and LV pacing sites to within 7 mm and 10 mm, respectively.

3.3 Atrial flutter (Fig. 4).

The previous section demonstrated ECGI's ability to map noninvasively ectopic focal activity and to locate the arrhythmogenic focus (**Fig. 3**). Another mechanism underlying cardiac arrhythmia is reentry, in which the activation front forms a closed pathway (the reentry circuit) that captures the heart. **Fig. 4** demonstrates the ability of ECGI to image noninvasively a reentry circuit during an atrial arrhythmia (atrial flutter). The anterior view shows the right atrial reentry circuit that drives the flutter (black arrows). The wavefront propagates up the septum (dashed arrow) and emerges near the Bachman bundle (asterisk). It then propagates down the free wall and reenters the septum through the isthmus between the inferior vena cava (IVC) and tricuspid annulus (TA). This primary circuit generates many secondary excitation waves that spread in all directions. A major wavefront propagates around the IVC (white arrow in inferior IVC view) and ascends the lateral right atrium (white arrow in right lateral view) to collide at the crista terminalis region with a leftward front (gray arrows) that emerges from the reentry circuit (black arrow). Other wavefronts (gray arrows; posterior, anterior and right lateral views) that emanate from the reentry circuit propagate to the left atrium, with the left atrial appendage being last to activate. This reentry circuit and activation pattern, mapped noninvasively using ECGI, is consistent with results from direct mapping of typical atrial flutter using intracardiac catheters [27-29].

4. DISCUSSION

Cardiac arrhythmias are a major cause of death and disability, with many mortalities occurring suddenly without prior warning. There is clearly a need for a noninvasive imaging modality for cardiac electrophysiology and arrhythmia that could be used for (1) screening people for risk of life threatening arrhythmias so that prophylactic measures can be taken; (2) specific diagnosis of the arrhythmia type and its mechanism to determine suitable intervention; (3) determination of the arrhythmogenic substrate and its location to guide localized intervention (such as ablation, pacing, targeted drug delivery and gene transfer); (4) follow-up and evaluation of efficacy of therapy. In addition to these clinical applications, such noninvasive modality could be used to study the properties and mechanisms of cardiac arrhythmias in humans, where the electrophysiological substrate differs markedly from that in animal models used thus far in arrhythmia research.

The results reviewed here demonstrate the ability of ECGI to reconstruct images of cardiac electrical activity on the epicardial surface of the human heart. We provide examples of normal activation and repolarization, ventricular pacing, and atrial flutter. The normal images are consistent with published invasive maps in the chimpanzee [23] and human [19]. Pacing serves to simulate an arrhythmia of focal origin (the pacing site); ECGI located RV and LV pacing sites to within 7 mm and 11 mm of their actual location (determined by CT). The atrial flutter images mapped detail of the reentry circuit responsible for the arrhythmia and its different components (e.g., an area of slow conduction in the narrow isthmus between the IVC and tricuspid annulus which could be a target for ablation). In addition, details of activation fronts emanating from the main circuit were obtained by ECGI, including wavefront collisions at the crista terminalis and late activation of the LA.

It is our hope that ECGI will develop into a clinical tool for the diagnosis and treatment of cardiac arrhythmias. We also believe that it could become a powerful tool for mechanistic studies of human cardiac electrophysiology and rhythm disorders of the heart.

ACKNOWLEDGEMENTS

The work summarized in this article was supported by a Merit Award R37-HL-33343 and grant R01-HL-49054 from the NIH – National Heart, Lung and Blood Institute. Y. Rudy is the Fred Saigh Distinguished Professor of Engineering at Washington University in St. Louis.

REFERENCES

1 Ramanathan C, Ghanem RN, Jia P, Ryu K, Rudy Y, "Noninvasive electrocardiographic imaging for cardiac electrophysiology and arrhythmia", Nat Med. **10**, 422-8, 2004.

2 Barr RC and Spach, M.S. Inverse solutions directly in terms of potentials. In: *The Theoretical Basis of Electrocardiography*, 294, eds. Nelson CV and Geselowirz, DB., Clarendon Press, Oxford, 1976.

3 Franzone PC, Taccardi B, Viganotti C, "An approach to inverse calculation of epicardial potentials from body surface maps" Adv Cardiol., **21**, 50-4, 1978.

4 Yamashita Y, " Inverse solution in electrocardiography: determining epicardial from body surface maps by using the finite element method", Jpn Circ J., **45**, 1312-22, 1981.

5 Rudy Y, Messinger-Rapport BJ, "The inverse problem in electrocardiography: solutions in terms of epicardial potentials", Crit Rev Biomed Eng, **16**, 215-68, 1988.

6 Brebbia CA, Telles JCF, Wrobel LC. *Boundary Element Techniques: Theory and Applications in Engineering*. Springer-Verlag ,Berlin, 1984.

7 Tikhonov AN, Arsenin VY. *Solutions of Ill-posed Problems*. Wiley , New York, 1977.

8 Ramanathan C, Jia P, Ghanem R, Calvetti D, Rudy Y, "Noninvasive electrocardiographic imaging (ECGI): application of the generalized minimal residual (GMRes) method", Ann Biomed Eng, **31**, 981-94, 2003.

9 Calvetti D, Lewis B, Reichel L, "Gmres, L curves, and discrete ill-posed problems", BIT, **42**, 44-65, 2002.

10 Messinger-Rapport BJ, Rudy Y, "Noninvasive recovery of epicardial potentials in a realistic heart-torso geometry. Normal sinus rhythm", Circ Res, **66**, 1023-39, 1990.

11 Oster HS, Taccardi B, Lux RL, Ershler PR, Rudy Y, "Noninvasive electrocardiographic imaging: reconstruction of epicardial potentials, electrograms, and isochrones and localization of single and multiple electrocardiac events" Circulation, **96**, 1012-24, 1997.

12 Oster HS, Taccardi B, Lux RL, Ershler PR, Rudy Y, "Electrocardiographic imaging: Noninvasive characterization of intramural myocardial activation from inverse-reconstructed epicardial potentials and electrograms", Circulation, **97**, 1496-507, 1998.

13 Burnes JE, Taccardi B, MacLeod RS, Rudy Y, "Noninvasive ECG imaging of electrophysiologically abnormal substrates in infarcted hearts: A model study", Circulation, **101**, 533-40, 2000.

14 Burnes JE, Taccardi B, Rudy Y, "A noninvasive imaging modality for cardiac arrhythmias", Circulation, **102**, 2152-8, 2000.

15 Burnes JE, Taccardi B, Ershler PR, Rudy Y, "Noninvasive electrocardiogram imaging of substrate and intramural ventricular tachycardia in infarcted hearts", J Am Coll Cardiol, **38**, 2071-8, 2001.

16 Ghanem RN, Burnes JE, Waldo AL, Rudy Y, "Imaging dispersion of myocardial repolarization, II: noninvasive reconstruction of epicardial measures", Circulation, **104**, 1306-12, 2001.

17 Ghanem RN, Jia P, Ramanathan C, Ryu K, Markowitz A, Rudy Y, "Noninvasive electrocardiographic imaging (ECGI): comparison to intraoperative mapping in patients", Heart Rhythm, **2**, 339-54, 2005.

18 Intini A, Goldstein RN, Jia P, Ramanathan C, Ryu K, Giannattasio B, Gilkeson R, Stambler BS, Brugada P, Stevenson WG, Rudy Y, Waldo AL, "Electrocardiographic imaging (ECGI), a novel diagnostic modality used for mapping of focal left ventricular tachycardia in a young athlete", Heart Rhythm, **2**, 1250-2, 2005.

19 Durrer D, van Dam RT, Freud GE, Janse MJ, Meijler FL, Arzbaecher RC, "Total excitation of the isolated human heart", Circulation, **41**, 899-912, 1970.

20 Arisi G, Macchi E, Baruffi S, Spaggiari S, Taccardi B, "Potential fields on the ventricular surface of the exposed dog heart during normal excitation", Circ Res, **52**, 706-15, 1983.
21 Wyndham CR, Meeran MK, Smith T, Saxena A, Engelman RM, Levitsky S, Rosen KM, "Epicardial activation of the intact human heart without conduction defect", Circulation, **59**, 161-8, 1979.
22 Kupersmith J, "Electrophysiologic mapping during open heart surgery", Prog Cardiovasc Dis, **19**, 167-202, 1976.
23 Spach MS, Barr RC, Lanning CF, Tucek PC, "Origin of body surface QRS and T wave potentials from epicardial potential distributions in the intact chimpanzee", Circulation, **55,** 268-8, 1977.
24 Jouve A, Corriol J, Torresani J, Benyamine R, Velasque P, Peytavy R, "Epicardial leads in man", Am Heart J, **59**, 856-68, 1960.
25 Roos JP, van Dam RT, Durrer D, "Epicardial and intramural excitation of normal heart in six patients 50 years of age and older", Br Heart J, **30**, 630-7, 1968.
26 Lux RL, Green LS, MacLeod RS, Taccardi B, "Assessment of spatial and temporal characteristics of ventricular repolarization", J Electrocardiol, **27** Suppl, 100-5, 1994.
27 Yamabe H, Misumi I, Fukushima H, Ueno K, Kimura Y, Hokamura Y, "Conduction properties of the crista terminalis and its influence on the right atrial activation sequence in patients with typical atrial flutter", Pacing Clin Electrophysiol, **25**, 132-41, 2002.
28 Daoud EG, Morady F, "Pathophysiology of atrial flutter", Annu Rev Med, **49**, 77-83, 1998.
29 Rodriguez LM, Timmermans C, Nabar A, Hofstra L, Wellens HJ, "Biatrial activation in isthmus-dependent atrial flutter", Circulation, **104**, 2545-50, 2001.

FIGURE LEGENDS

Figure 1. **A block diagram of the ECGI procedure**. **(a)** Multielectrode vest for obtaining ECGs and CT for obtaining geometry. **(b)** CT slices showing heart contour (red) and body-surface electrodes (shiny dots). **(c)** Heart-torso geometry constructed from the CT slices. **(d)** Sample ECGs obtained with the multielectrode vest and mapping system. **(e)** Body surface potential map. **(f)** ECGI software, CADIS, for reconstruction of epicardial potentials. **(g)** Examples of noninvasive ECGI images: epicardial potentials, electrograms and isochrones. From reference [1]. A color version of this figure is available in the symposium CD-ROM proceedings.

Figure 2. **Ventricular activation of a normal subject**. **(a)** Left, anterior and posterior views of body surface potential map, 35 ms after QRS onset. Lead V2 of standard ECG is shown for timing purposes. Right, noninvasive epicardial potential map reconstructed from BSPM at left. RV, right ventricle; LV, left ventricle; LAD, left anterior descending coronary artery; LA, left atrium; RA, right atrium. **(b)** Left, epicardial electrograms from locations 1, 5, 3 and 4 (shown in **a**, right). Right, epicardial isochrones. 1, 2,3 and 4 indicate locations of early epicardial activation (breakthrough sites). From reference [1]. A color version of this figure is available in the symposium CD-ROM proceedings.

Figure 3. **Ventricular activation during RV (top) and LV (bottom) pacing**. **(a)** Anterior views of epicardial potential map during RV pacing. Left, translucent view showing pacing lead. Right, opaque view showing minimum at pacing site location **(*)**. Anterior view is tilted 10° to show pacing site location on inferior RV apex. **(b)** Anterior and posterior views of epicardial isochrone map for RV pacing. Electrograms from three locations are shown at their respective spatial locations. **(c)** Posterior views of epicardial potential map during LV pacing (same format as in **a**). **(d)** Epicardial isochrone map with electrograms for LV pacing (same format as in **b**). LAD, left anterior descending coronary artery; LA, left atrium; RA, right atrium. From reference [1]. A color version of this figure is available in the symposium CD-ROM proceedings.

Figure 4. **ECGI images of atrial flutter**. Isochrone maps are shown. The right atrial reentry circuit that drives the flutter is indicated by black arrows. RAFW, right atrial free wall; LAA, left atrial appendage; SVC, superior vena cava; TA, tricuspid annulus; MA, mitral annulus; PV, pulmonary vein; SEP, septum; CrT, crista terminalis. From reference [1]. A color version of this figure is available in the symposium CD-ROM proceedings.

FIGURES

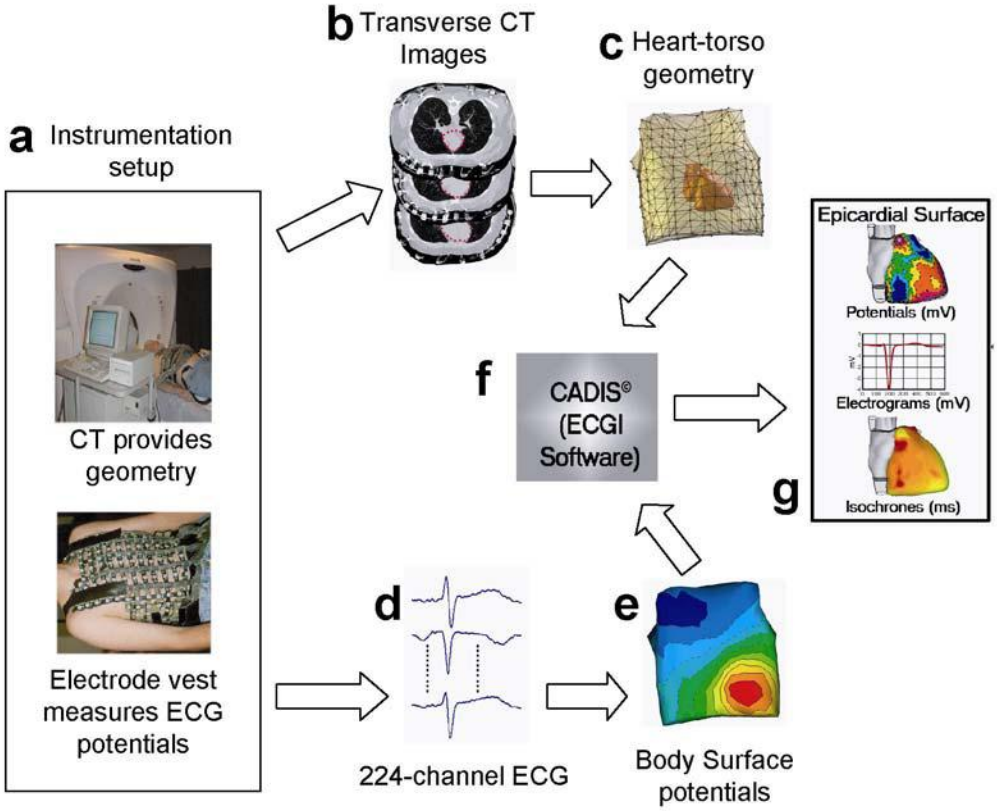

Figure 1. A block diagram of the ECGI procedure.

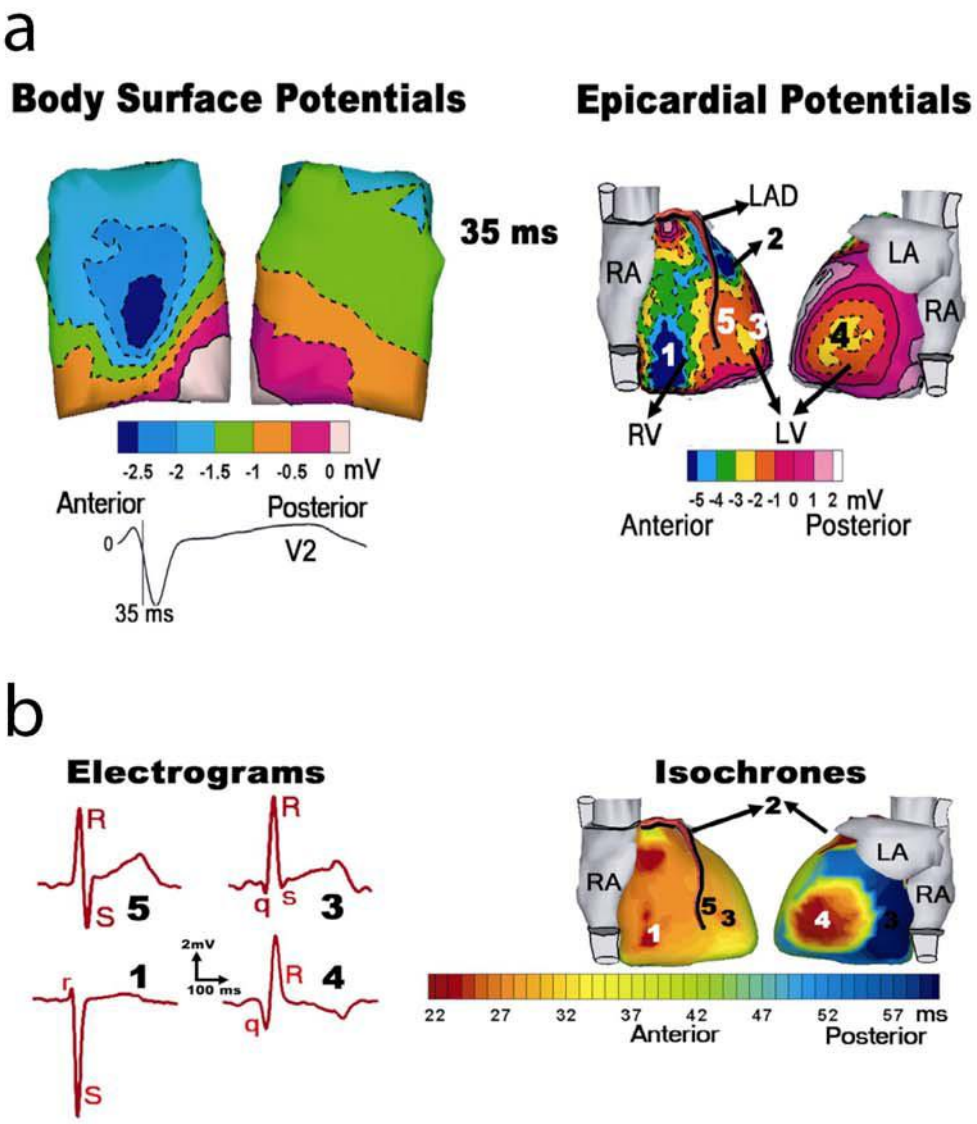

Figure 2. Ventricular activation of a normal subject.

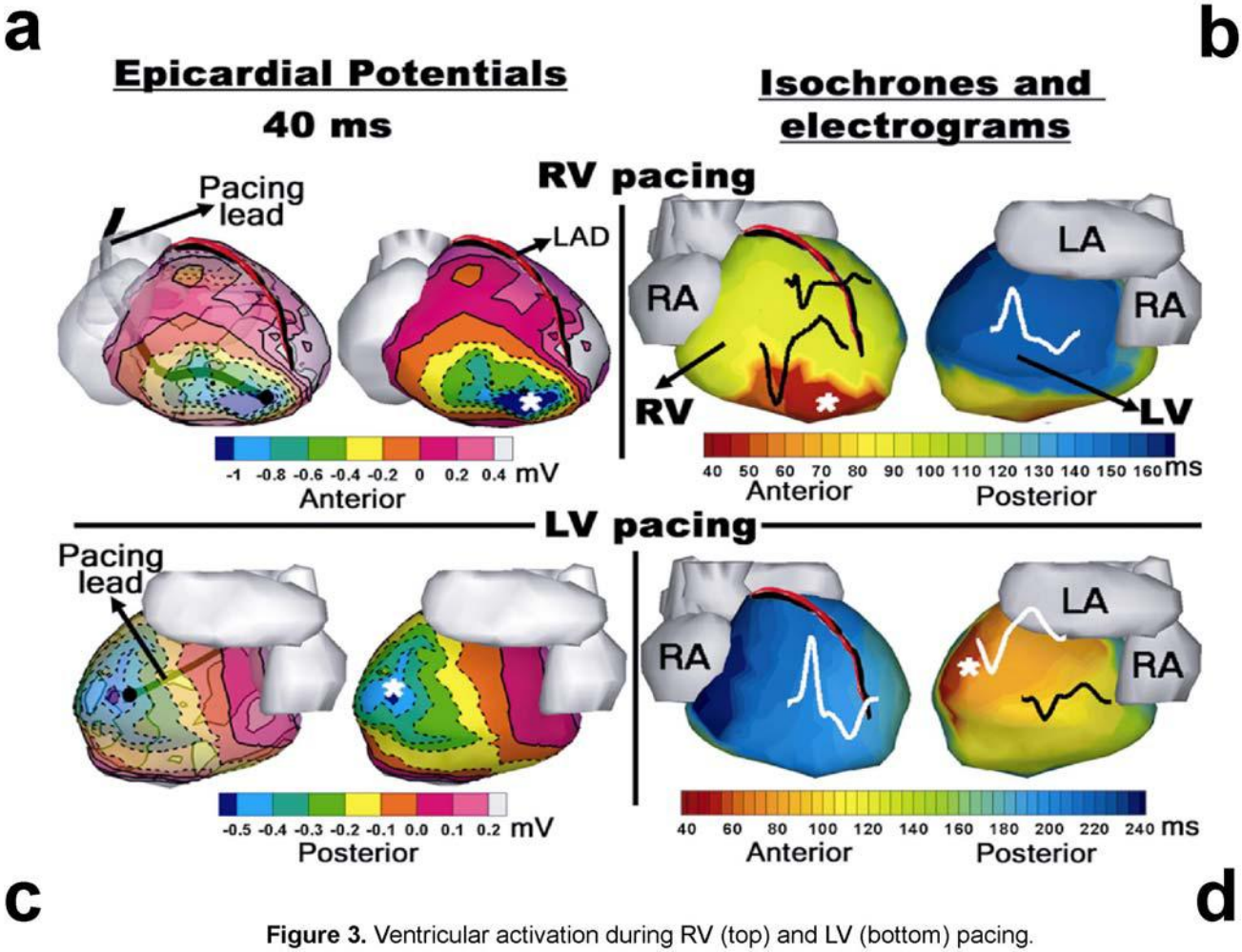

Figure 3. Ventricular activation during RV (top) and LV (bottom) pacing.

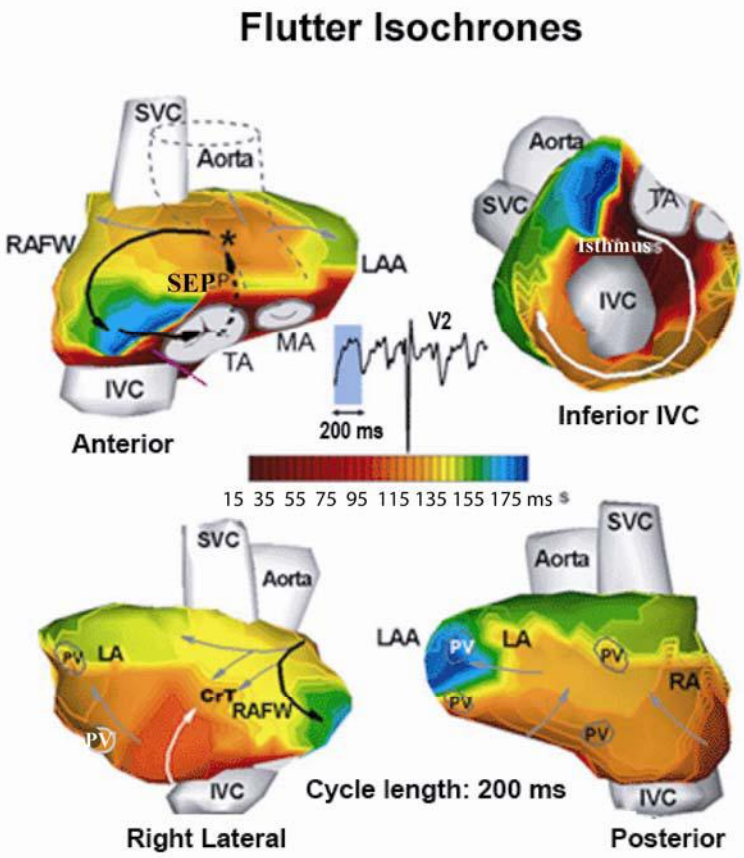

Figure 4. ECGI images of atrial flutter.